

UDK 546.714:675.017.5

Influence of Mn Site Doping on Electrical Resistivity of Polycrystalline $\text{La}_{1-y}\text{A}_y\text{Mn}_{1-x}\text{B}_x\text{O}_3$ (A=Ba, Sr; B=Cu, Cr, Co) Manganites

N. Paunović^{1*)}, Z. V. Popović¹, A. Cantarero², F. Sapina²

¹Center for Solid State Physics and New Materials, Institute of Physics, P.O. Box 68, 11080 Belgrade, Serbia

²Materials Science Institute, University of Valencia, P. O. Box 22085, 46071 Valencia, Spain

Abstract:

We have the measured electrical resistivity of $\text{La}_{1-y}\text{Ba}_y\text{Mn}_{1-x}\text{Cu}_x\text{O}_3$ ($0.17 \leq y \leq 0.30$; $0.04 \leq x \leq 0.10$), $\text{La}_{1-y}\text{Sr}_y\text{Mn}_{1-x}\text{Cr}_x\text{O}_3$ and $\text{La}_{1-y}\text{Sr}_y\text{Mn}_{1-x}\text{Co}_x\text{O}_3$ ($0.270 \leq y \leq 0.294$; $0.02 \leq x \leq 0.10$) polycrystalline samples in the 25-325 K temperature range. The increase of Mn site doping concentration leads to an increase of the electrical resistivity of the samples and the appearance of a “double-peak” structure in the electrical resistivity versus temperature graphs. The first peak represents the insulator-metal transition in vicinity of the paramagnetic-ferromagnetic transition (T_C). We have found that the intensity of the second peak increases with an increase of concentration of Mn substituents, due to the hole scattering by the random potential of the Mn site impurities.

Keywords: Manganites, Colossal magnetoresistance, Electrical resistivity.

Introduction

Manganites with general formula $\text{R}_{1-x}\text{A}_x\text{MnO}_3$ where R is a rare earth metal like La, Pr, Nd or Dy and A is an alkaline-earth metal like Sr, Ca, Ba or Pb, have attracted much attention since 1994, when S. Jin et al. [1] discovered so called colossal magnetoresistance (CMR) in $\text{La}_{0.67}\text{Ca}_{0.33}\text{MnO}_3$ of about 100000%. These materials are interesting for applications as magnetic field sensors or magnetic data storage devices and especially in spintronics as efficient injectors of spin polarized electrons due to their fully spin polarized e_g bands. Beside practical applications, manganites with CMR are also interesting because of their very rich phase diagram, which is a consequence of strong interplay between spin, charge, orbital and lattice degrees of freedom.

Manganites with CMR have the paramagnetic-ferromagnetic (PM-FM) transition at Curie temperature T_C . The typical electrical resistivity vs temperature curve of these materials shows an insulator behavior above T_C and metallic behavior below T_C . Partial substitution of the rare earth (R-element) with a divalent element (A) converts a proportional number of Mn^{3+} ions into Mn^{4+} ions and introduces free electrons into the e_g band, enabling the double

*) Corresponding author: npaun@phy.bg.ac.yu

exchange (DE) mechanism [2], which is traditionally used for a basic qualitative explanation of unusual transport and magnetic properties of these materials. Further studies on these materials have shown that electron-phonon interaction in the form of Jahn-Teller polarons, the orbital ordering, the electron-electron correlations and the coupling between spin and orbital structure can also play a very important role [3].

Polycrystalline CMR manganites exhibit considerably different behavior than single crystal samples. For single crystals and epitaxial films a very large magnetoresistance ratio exists only for temperatures close to T_C and in high magnetic fields. On the other hand, polycrystalline samples show a considerable magnetoresistance ratio over a wide temperature range below T_C and in a rather low magnetic field. This finding has been explained with spin-polarized intergrain tunneling [4,5]. Electrical resistivity of some polycrystalline samples showed a “double-peak” structure [5-10], which has been attributed to the existence of a disordered shell at the surface of the grains [5,7]. In this paper we have measured electrical resistivity of $\text{La}_{1-y}\text{Ba}_y\text{Mn}_{1-x}\text{Cu}_x\text{O}_3$ ($0.17 \leq y \leq 0.30$; $0.04 \leq x \leq 0.10$), $\text{La}_{1-y}\text{Sr}_y\text{Mn}_{1-x}\text{Cr}_x\text{O}_3$ and $\text{La}_{1-y}\text{Sr}_y\text{Mn}_{1-x}\text{Co}_x\text{O}_3$ ($0.270 \leq y \leq 0.294$; $0.02 \leq x \leq 0.10$) polycrystalline samples in the 25-325 K temperature range. The samples showed the double-peak electrical resistivity behavior. The peak below T_C increases intensity with an increase of concentration of Mn substituents. This is explained as a consequence of Mn-O-Mn network strain and scattering by the random potential introduced by Mn substitution.

Experiment

Single-phase $\text{La}_{1-y}\text{Ba}_y\text{Mn}_{1-x}\text{Cu}_x\text{O}_3$ ($0.17 \leq y \leq 0.30$; $0.04 \leq x \leq 0.10$), $\text{La}_{1-y}\text{Sr}_y\text{Mn}_{1-x}\text{Cr}_x\text{O}_3$ and $\text{La}_{1-y}\text{Sr}_y\text{Mn}_{1-x}\text{Co}_x\text{O}_3$ ($0.270 \leq y \leq 0.294$; $0.02 \leq x \leq 0.10$) polycrystalline samples have been prepared via the acetic acid solution freeze-drying method. This soft procedure makes possible strict stoichiometric control, and the synthetic variables allow one to maintain the proportion of Mn^{4+} at constant and optimal value of $\sim 32\%$ at which the CMR effect is the strongest. In this way, the concentration of cationic vacancies at La and Mn sites is practically negligible in all cases. X-ray powder diffraction patterns for all samples have been completely indexed and refined with rhombohedral perovskite symmetry and the $R\bar{3}c$ space group. Details on the preparation of the samples, together with X-ray diffraction and magnetization measurements can be found in Ref. [11].

For electrical resistivity measurements four golden spots were evaporated on disk-shaped ceramic pellets. These golden contacts were connected with the measuring unit using golden wires. The low temperature electrical resistivity measurements were realized using a Displex model ARS - DE-202N closed cycle helium cryostat with the van der Pauw technique.

Results and discussion

Fig. 1 shows the temperature dependence of electrical resistivity of $\text{La}_{1-y}\text{Ba}_y\text{Mn}_{1-x}\text{Cu}_x\text{O}_3$ ($0.17 \leq y \leq 0.30$; $0.04 \leq x \leq 0.10$) polycrystalline samples in the 25-325 K temperature range. With temperature decrease the samples undergo a paramagnetic to ferromagnetic transition (at T_C) accompanied with an insulator to metal (IM) transition (at T_{IM}) in the vicinity of T_C . As the Mn doping level x increases, T_C decreases as a consequence of the weakening of the DE interaction due to the crystal distortion and perturbation of the connecting paths for the transport of holes across Mn-O-Mn chains (structural disorder introduced by large substitutional cations [11]). Overall electrical resistivity of samples increases with increasing x as a consequence of hole scattering by random potential

introduced by Mn-ion substitution. For $x=0.10$ Cu doped sample a combination of crystal distortion and scattering caused by Cu is strong enough to completely inhibit the IM transition, as it is shown in the inset in Fig. 1.

The most interesting feature in Fig. 1 is the appearance of a very broad peak at temperature T_2 (below T_C). The double-peak structure in electrical resistivity vs temperature graphs has been previously observed in some polycrystalline samples [5-10,12]. Several scenarios were proposed to describe the double-peak structure. In Ref. [5,7], it was suggested that the crystal grains consist of two phases, a highly crystalline core with properties similar to single crystals, and a surface phase (at grain boundary regions), which due to its lower stoichiometry, higher amorphization and strain induced disorder, has weaker DE and hence lower T_C and higher electrical resistivity. In this interpretation the peak at T_{IM} originates from the core phase, whereas the second peak at T_2 originates from the surface phase. The so-called "phase separation" concept [13] has also been used to explain this phase transition. In the present case, two types of ferromagnetic phase exist: one is metallic (FMM) and the second one insulating (FMI). The FMM state is gradually destroyed by Mn site substitution, and the magnetic spontaneous state is driven into a cluster state. On lowering the temperature, FM clusters grow up and an insulator/metal transition at T_2 can be explained by percolative transport through ferromagnetic metallic domains. In Ref. [12] we proposed that the double peak structure in the temperature dependence of electrical resistivity can be a consequence of a competition between the short range orbital/charge order and the long range FM order.

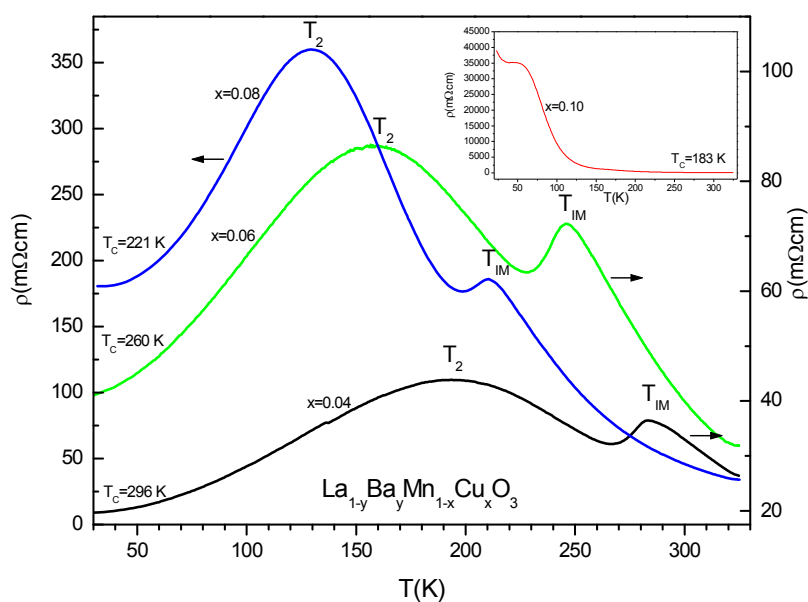


Fig. 1 Temperature dependence of electrical resistivity of $\text{La}_{1-y}\text{Ba}_y\text{Mn}_{1-x}\text{Cu}_x\text{O}_3$ polycrystalline samples in the 25-325 K temperature range. Inset: resistivity vs. temperature of the $x=0.10$ sample.

In our samples we have substitution of Mn with various elements. It is clear that with increase of Cu doping, Fig. 1, the intensity of the second peak increases and shifts to lower temperatures. We also noted that the difference between T_2 and T_C is almost constant with changing of x : $T_C - T_2 \approx 100$ K, indicating correlation between T_2 and T_C (Fig. 2).

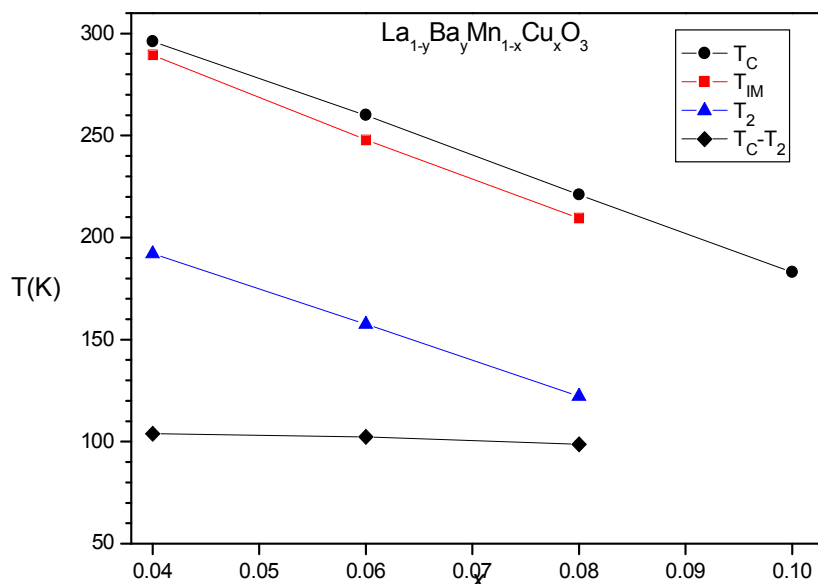


Fig. 2 Values of T_C , T_{IM} , T_2 and $T_C - T_2$ for different doping concentrations x of the $La_{1-y}Ba_yMn_{1-x}Cu_xO_3$ sample.

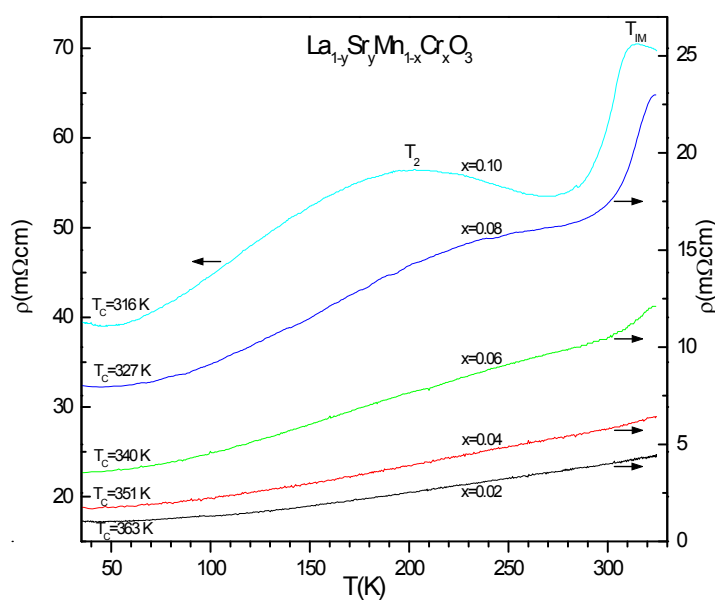


Fig. 3 Temperature dependence of electrical resistivity of $La_{1-y}Sr_yMn_{1-x}Cr_xO_3$ polycrystalline samples in the 25-325 K temperature range.

Fig. 3 and 4 show the temperature dependence of electrical resistivity of $La_{1-y}Sr_yMn_{1-x}Cr_xO_3$ and $La_{1-y}Sr_yMn_{1-x}Co_xO_3$ ($0.270 \leq y \leq 0.294$; $0.02 \leq x \leq 0.10$). $La_{1-y}Sr_yMnO_3$ samples have the highest T_C among CMR manganites. In the measured 25-325 K temperature range we can clearly see the IM transition only for samples with the highest Mn site doping level, when T_C is reduced enough. These electrical resistivity spectra also show the double-peak behavior, but the second peak is less pronounced than in the case of Cu doped samples.

The second peak is the strongest for the Cr doped sample with $x=0.10$. However, it can be concluded that the intensity of the second peak increases and the peak shifts to lower temperatures with an increase of Cr and Co content, as in the case of Cu doped samples.

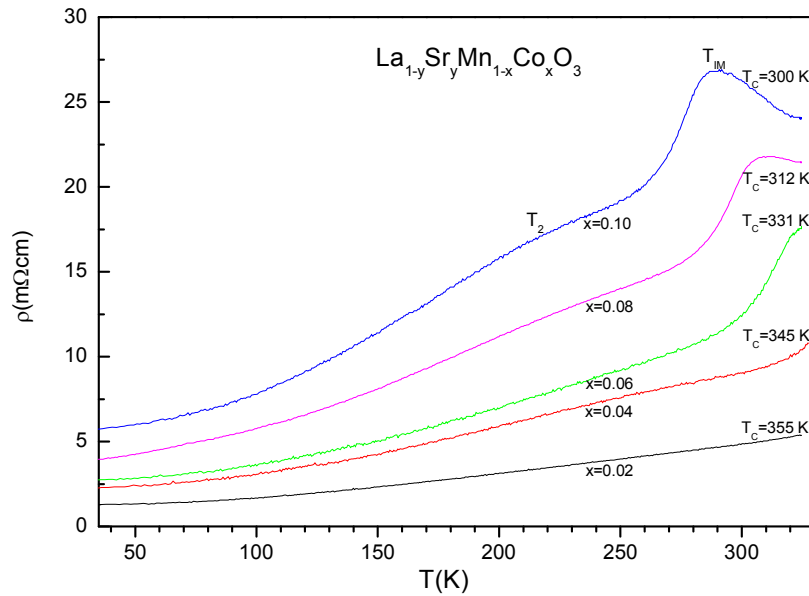


Fig. 4 Temperature dependence of electrical resistivity of $\text{La}_{1-y}\text{Sr}_y\text{Mn}_{1-x}\text{Co}_x\text{O}_3$ polycrystalline samples in the 25-325 K temperature range.

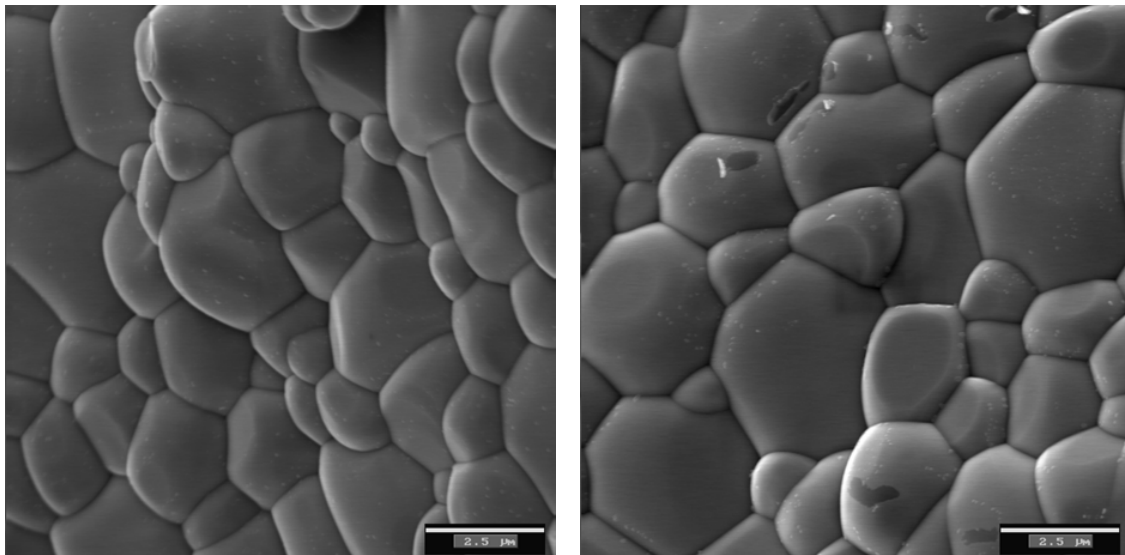


Fig. 5 SEM images of $\text{La}_{1-y}\text{Ba}_y\text{Mn}_{1-x}\text{Cu}_x\text{O}_3$ samples for $x=0.04$ (left) and $x=0.08$ (right).

Surthi et al. [7] investigated the influence of grain size on the second (broad) peak in polycrystalline $\text{La}_{0.67}\text{Ca}_{0.33}\text{MnO}_3$ and showed that the intensity of this peak increases with a decrease of grain size due to increased influence of the surface phase in smaller grains. In Fig. 5 SEM images of Cu doped samples for $x=0.04$ and $x=0.08$ are given, showing a similar overall grain size and morphology. Thus, in our samples the grain size cannot be the reason for the intensity increase of the second peak. We believe that the intensity increase of the

second electrical resistivity peak is most likely due to the combination of Mn-O-Mn network strain and scattering by the random potential introduced by Mn substitution. Substitution of Mn by large cations reduces the Mn-O-Mn angle and weakens the DE interaction, which hampers hopping of e_g electrons responsible for conductivity. Ionic radii of Cr^{3+} (75.5 pm) and Co^{3+} (75 pm) are very similar to the mean radius of $\text{Mn}^{3+}/\text{Mn}^{4+}$ ions (75.05 pm), while Cu^{2+} has a significantly larger ionic radius (87 pm) [14]. Accordingly, the substitution of Mn by Cu has a much stronger effect on the intensity increase of the second peak than substitution by Cr and Co. Mismatch of oxidation states between $\text{Mn}^{3+}/\text{Mn}^{4+}$ and substituent cations is also likely to have a contribution to the second peak intensity increase. Since the difference between oxidation states of $\text{Mn}^{3+}/\text{Mn}^{4+}$ (mean value 3.33) and Cu^{2+} is much bigger than the difference between $\text{Mn}^{3+}/\text{Mn}^{4+}$ and Cr^{3+} or Co^{3+} oxidation states, the Cu^{2+} ions are much stronger scatterers than Cr^{3+} or Co^{3+} .

Conclusions

We have measured the electrical resistivity of $\text{La}_{1-y}\text{Ba}_y\text{Mn}_{1-x}\text{Cu}_x\text{O}_3$ ($0.17 \leq y \leq 0.30$; $0.04 \leq x \leq 0.10$), $\text{La}_{1-y}\text{Sr}_y\text{Mn}_{1-x}\text{Cr}_x\text{O}_3$ and $\text{La}_{1-y}\text{Sr}_y\text{Mn}_{1-x}\text{Co}_x\text{O}_3$ ($0.270 \leq y \leq 0.294$; $0.02 \leq x \leq 0.10$) polycrystalline samples in the 25-325 K temperature range. The samples showed the double-peak electrical resistivity behavior. The peak below T_C increases intensity with an increase of concentration of Mn substituents. This is explained as a consequence of Mn-O-Mn network strain and scattering by the random potential introduced by Mn substitution.

Acknowledgments

This work was supported by the Serbian Ministry of Science under the project no 141047 and the Serbian Academy of Science and Art, project no. F-134.

References

1. S. Jin, T. H. Tiefel, M. McCormack, R. A. Fastnacht, R. Ramesh, L. H. Chen, *Science* 264 (1994) 413.
2. C. Zener, *Phys. Rev.* 81 (1951) 403.
3. A. J. Millis, R. Mueller and B. I. Shraiman, *Phys. Rev. B.* 54, (1996), 5405.
4. H. Y. Hwang, S-W. Cheong, N. P. Ong, and B. Batlogg, *Phys. Rev. Lett* 77 (1996) 2041.
5. N. Zhang, W. Ding, W. Zhong, D. Xing, Y. Du, *Phys. Rev. B* 56 (1997) 8138.
6. A. Gupta, G. Q. Gong, G. Xiao, P. R. Duncombe, P. Lecoeur, P. Trouilloud, Y. Y. Wang, V. P. Dravid, and J. Z. Sun, *Phys. Rev. B* 54 (1996) R15629.
7. S. Surthi, S. Kotru, R.K. Pandey, P. Fournier, *Solid State Commun.* 125 (2003) 107.
8. X. L. Wang, P. Gehringer, W. Lang, J. Horvat, H. K. Lu, S. X. Dou, *Solid State Commun.* 117 (2001) 53.
9. A. D. Hernandez, C. Hart, R. Escudero, O. Ares, *Physica B* 320 (2002) 64.
10. J. Y. Yu, S. Y. Zhang, G. H. Liu, H. Y. Wu, L. Wang, *Solid State Commun.* 142 (2007) 333.
11. Z. El-Fadli, M. Redouane Metni, F. Sapina, E. Martinez, J.V. Folgado, A. Beltran, *Chem. Mater.* 14 (2002) 688.
12. Z.V. Popović, A. Cantarero, W.H.A. Thijssen, N. Paunović, Z. Dohčević-Mitrović, F. Sapina, *J. Phys.: Condens. Matter* 17 (2005) 351.
13. E. Dagotto, *Nanoscale phase separation and colossal magnetoresistance* *The Physics*

of Manganites and Related Compounds (Springer Series in Solid-State Sciences vol 136, 2003) (Berlin: Springer)

14. R. D. Shannon, Acta Crystallogr. A 32, (1976) 751.

Садржај: У раду су приказана мерења електричне отпорности $La_{1-y}Ba_yMn_{1-x}Cu_xO_3$ ($0,17 \leq y \leq 0,30$; $0,04 \leq x \leq 0,10$), $La_{1-y}Sr_yMn_{1-x}Cr_xO_3$ и $La_{1-y}Sr_yMn_{1-x}Co_xO_3$ ($0,270 \leq y \leq 0,294$; $0,02 \leq x \leq 0,10$) поликристалних узорака на температурама од 25 до 325 К. Уочена су два пика (максимума) у температурним зависностима специфичне електричне отпорности: први, изолатор-метал прелаз у близини парамагнетик-феромагнетик прелаза (T_C) и други веома широк пик испод T_C . Установили смо да пик испод T_C постаје истакнутији са повећањем концентрације Mn супституената, што се може објаснити напрезањем Mn-O-Mn мреже и расејањем на насумичним потенцијалима узрокованим Mn супституцијом.

Кључне речи: Магнетит, колосална магнетна отпорност, електрична отпорност.
